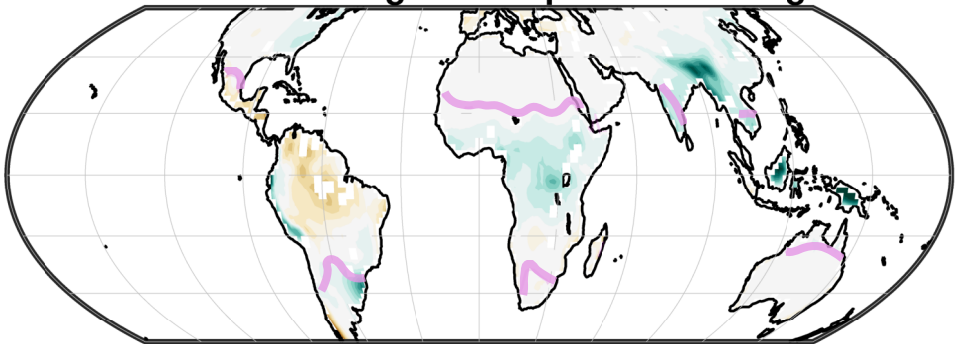


Figure.

# CMIP5/6 change in $P-E$ per 1K warming

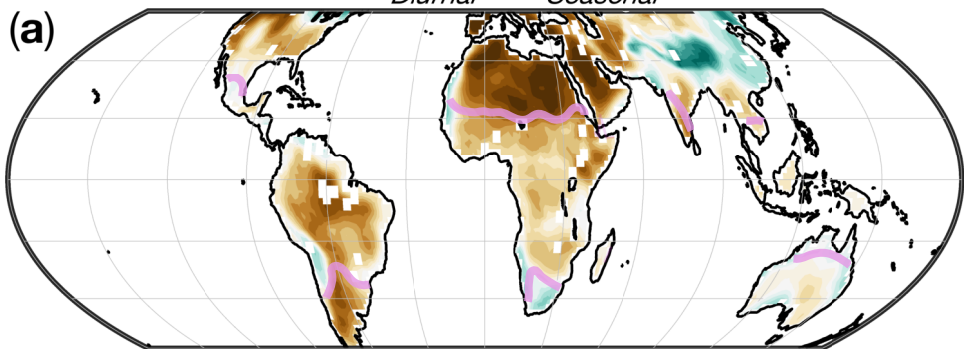


-0.4      -0.2      0      +0.2      +0.4

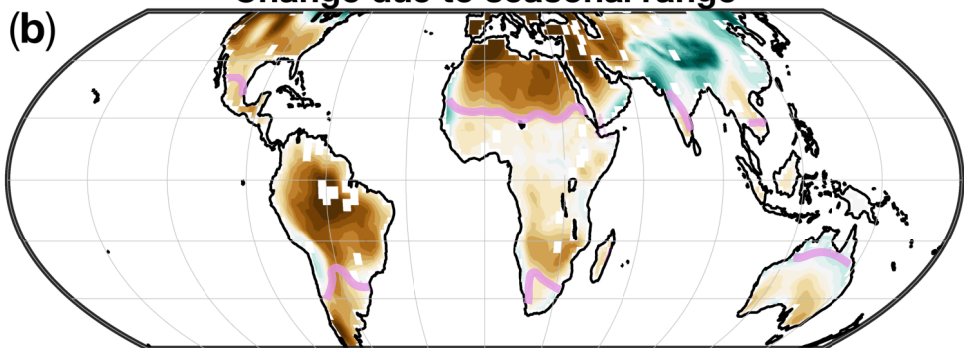
[mm day<sup>-1</sup> K<sup>-1</sup>]

Figure.

CMIP5/6 change in  $\Delta_{Diurnal} - \Delta_{Seasonal}$  per 1K warming



Change due to seasonal range



Change due to diurnal range

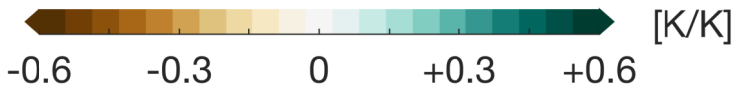
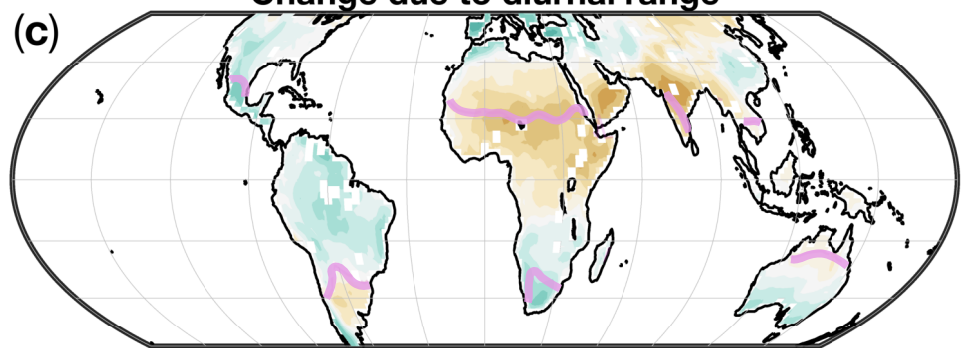


Figure.

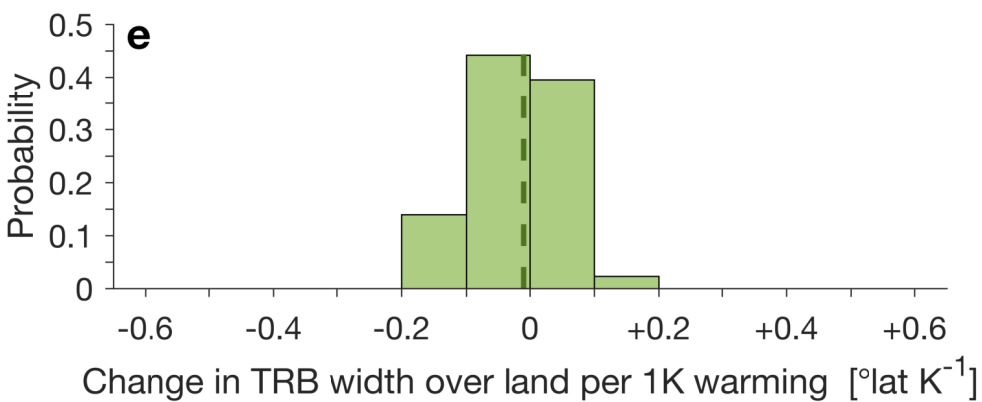
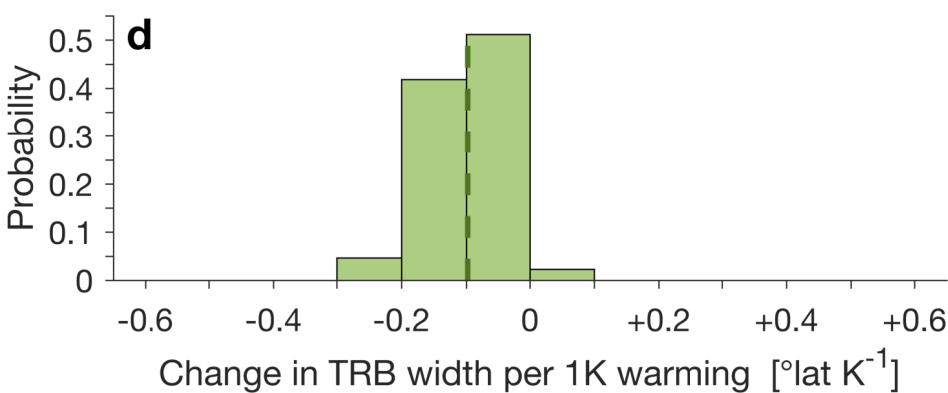
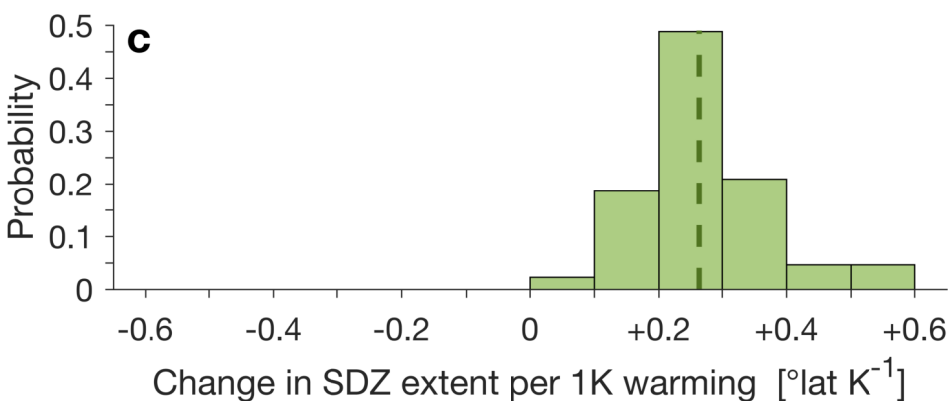
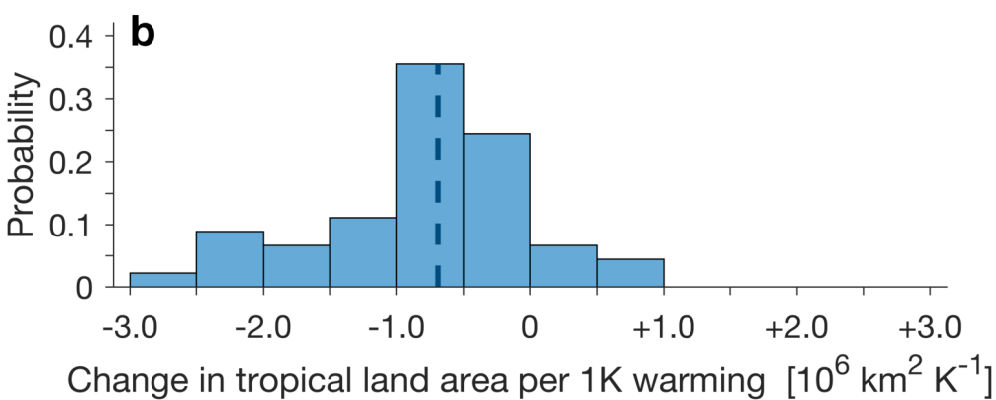
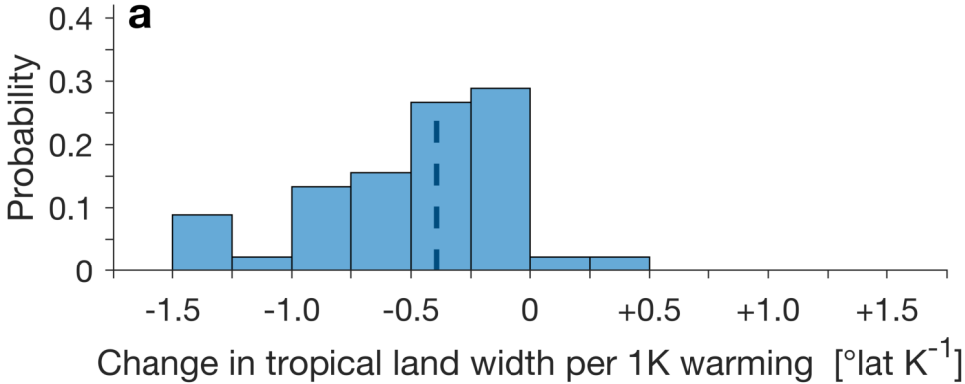


Figure.

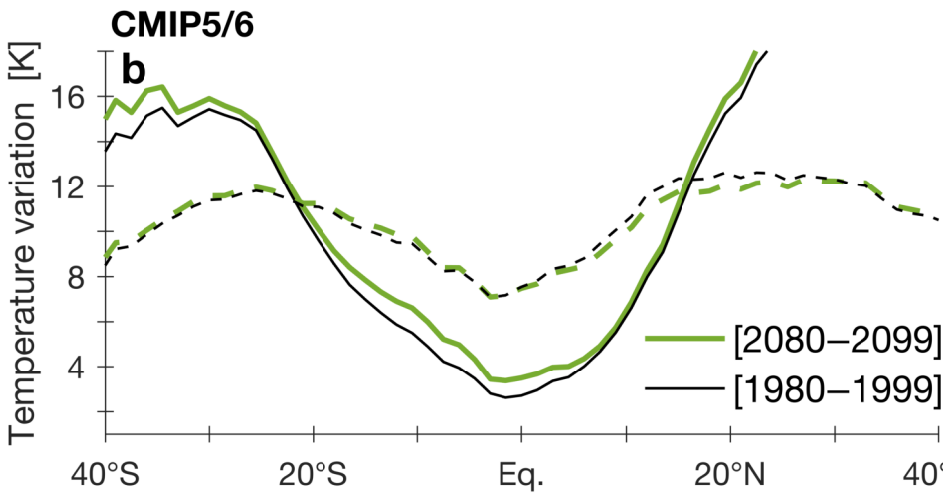
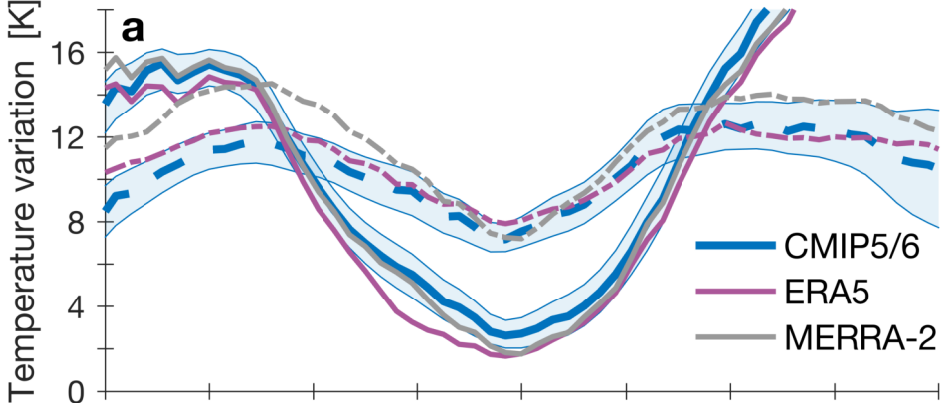
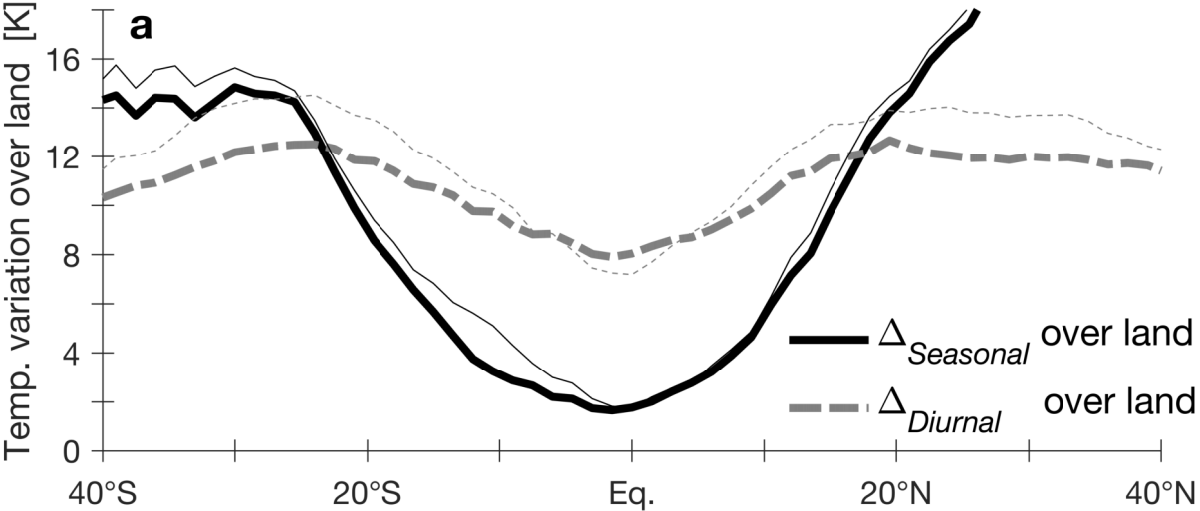
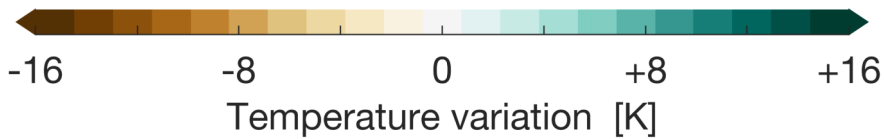
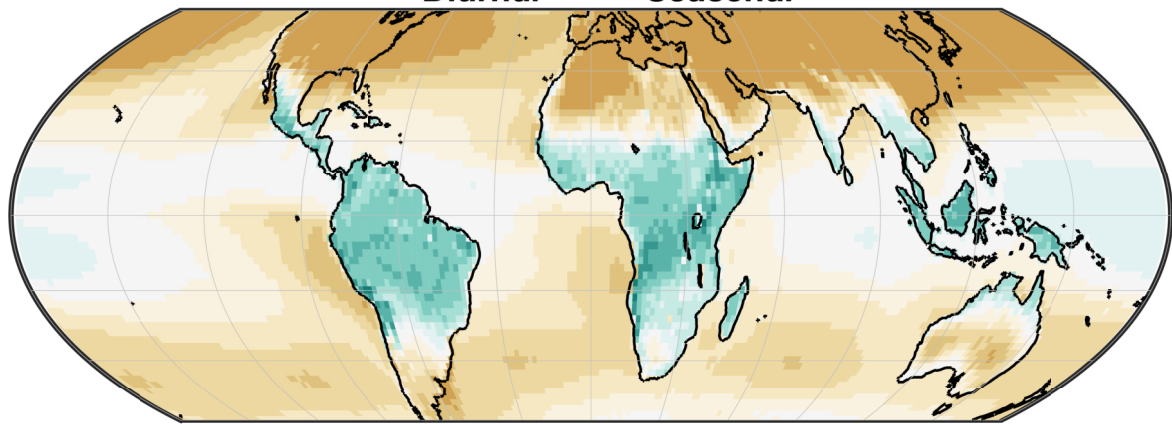


Figure.



**(b)**  $\Delta_{\text{Diurnal}} - \Delta_{\text{Seasonal}}$





## Abstract

Regions along the edges of the tropics host vast populations and ecosystems which are sensitive to climate change. Here we examine the extent of tropical climate land areas in the ERA5 and MERRA-2 reanalyses in high-emission scenarios of 45 models participating in phases 5 and 6 of the Coupled Model Intercomparison Project (CMIP5/6). Based on the definition of tropical climate land areas as regions where the diurnal temperature range exceeds the seasonal temperature range, we find a net reduction of tropical land area with global warming. This change is primarily due to an increased seasonal temperature range, driven by enhanced summer warming. The reduction in tropical land area is consistent with the expansion of the subtropical descending zones and with the expansion of drylands with global warming. However, the particular contributions of dynamic and thermodynamic processes are not clear.

## Plain Language Summary

Tropical climate land areas host about 40% of the world's population and 80% of the world's biodiversity. Changes in the extent of tropical climate land areas, which generally border semi-arid climate zones, can therefore carry vast ecological and socio-economic implications. Tropical climate land areas are generally defined as regions where the daily temperature range exceeds the seasonal temperature range. Based on this definition we find a net decrease in tropical land area in climate model projections of greenhouse-gas-induced global warming. The net reduction in tropical land area is driven primarily by increased seasonal temperature range, due to enhanced summer warming. The reduction in tropical land area is consistent with the expansion of the subtropical descending zones and with the expansion of drylands with global warming. However, the specific contributions of dynamic and hydrological processes are not clear.

## 1 Introduction

Tropical climate land areas host about 40% of the world's population and 80% of the world's biodiversity. Changes in the extent of tropical climate land areas, which generally border semi-arid climate zones, can therefore carry vast ecological and socio-economic implications (Ruane et al., 2021; Grünzweig et al., 2022). It is now well established that the tropical overturning circulation in the atmosphere has widened meridionally in recent decades, pushing subtropical dry zones poleward (Lu et al., 2007; Seidel et al., 2008), a tendency expected to continue under global warming (for reviews, see Staten et al., 2018, 2020). The extent of global drylands is similarly observed and projected to increase with global warming, partly at the expense of tropical land areas, due to increased global aridity (Feng & Fu, 2013; Huang et al., 2017). However, regional trends and the dynamic and thermodynamic drivers that underlie regional variations in the extent of the tropics remain poorly understood (Bony et al., 2015; Nguyen et al., 2018; Grise et al., 2018; Staten et al., 2019; Palmer & Stevens, 2019; D'Agostino et al., 2020). Here we analyze projected changes in the extent of tropical climate land areas using a simple definition of tropical zones based on temperature variations, and relate these changes to the expansion of the subtropical dry zones.

In the present climate, seasonal temperature variations nearly vanish near the equator and generally increase toward the poles – in accordance with seasonal insolation (Riehl et al., 1979). Diurnal temperature variations are similarly lower near the equator but vary modestly between tropical and subtropical latitudes (Riehl et al., 1979; Yang & Slingo, 2001). In addition, owing to the large contrast in heat capacity, tropical surface temperature variations over land are significantly larger than over ocean. Specifically, land variations are larger by a factor of about 10 on diurnal timescales, and by a factor of about 2 on seasonal timescales, making diurnal surface temperatures variations significantly larger than seasonal variations in the tropics (Riehl, 1954; Riehl et al., 1979). Tropical

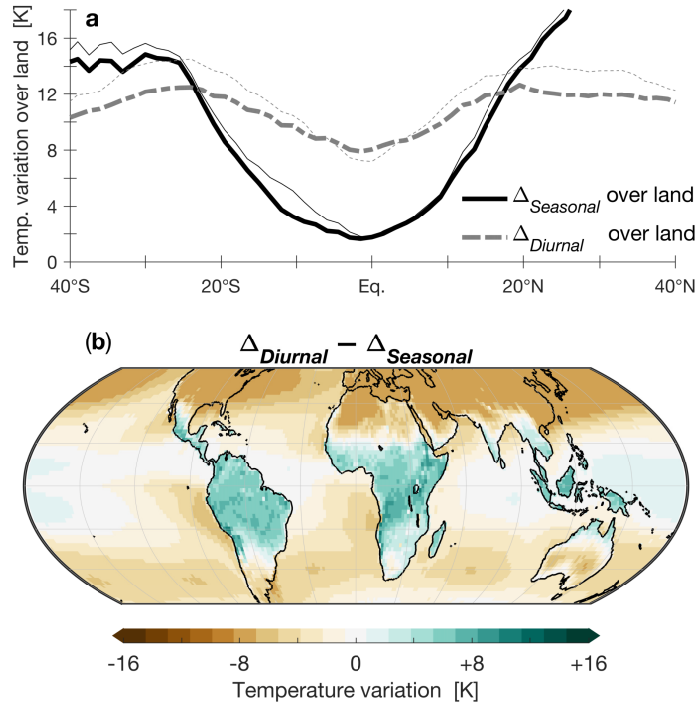


**Figure 1.** (a) Seasonal (solid black) and diurnal (dashed gray) surface temperature ranges ( $\Delta_{Seasonal}$  and  $\Delta_{Diurnal}$ , respectively), zonally averaged over land areas. (b) Global  $\Delta_{Diurnal} - \Delta_{Seasonal}$ . Data shown for climatological values of the European Centre for Medium-Range Weather Forecasts ERA5 dataset (panel b and thick lines in panel a, Hersbach et al., 2020), and for the National Aeronautics and Space Administration MERRA-2 dataset (thin lines in panel a, Gelaro et al., 2017), for the years 1980–2020. See section 2 for details on the data and calculations.

65 climate land areas are therefore conveniently defined as land regions where the diurnal  
 66 temperature range exceeds the seasonal temperature range – a definition commonly at-  
 67 tributed to Riehl et al. (1979), but first proposed by Troll (1943) and demonstrated in  
 68 Paffen (1967).

69 Figure 1 shows the observed climatological mean differences over land between max-  
 70 imal and minimal diurnal surface air temperatures ( $\Delta_{Diurnal}$ ) and between the hottest  
 71 and coldest months in each year ( $\Delta_{Seasonal}$ ). Tropical climate land areas, where  $\Delta_{Diurnal} >$   
 72  $\Delta_{Seasonal}$ , are clearly delineated from subtropical areas, with mean edges at about 24°S  
 73 and 17°N. Changes associated with global warming in the extent of tropical land areas,  
 74 as defined above, thus depend on the responses of seasonal and diurnal surface temper-  
 75 ature variations.

76 The sensitivities of seasonal and diurnal temperature variability to global warm-  
 77 ing have been extensively analyzed in modeling and observational studies (e.g., Stouf-  
 78 fer & Wetherald, 2007; Manabe et al., 2011; Sobel & Camargo, 2011; Dwyer et al., 2012;  
 79 Stine & Huybers, 2012; Donohoe & Battisti, 2013; Holmes et al., 2016; Yettella & Eng-  
 80 land, 2018; Chen et al., 2019). In high latitudes, the seasonal temperature range gener-  
 81 ally decreases with global warming due to enhanced winter warming (e.g., Manabe et  
 82 al., 2011; Dwyer et al., 2012; Chen et al., 2019). The diurnal temperature range has like-  
 83 wise generally decreased globally over the past century, especially in higher latitudes, due

84 to enhanced nighttime warming (Wild, 2009; Thorne, Menne, et al., 2016; Thorne, Do-  
85 nat, et al., 2016; K. Wang & Clow, 2020).

86 In contrast, at low latitudes global warming is associated with a weak general in-  
87 crease in both seasonal and diurnal surface temperature variability. The increase in the  
88 seasonal temperature range is mainly attributed to reduced evaporative cooling during  
89 summer, caused by decreased relative humidity and weakened circulation (Sobel & Ca-  
90 margo, 2011; Chen et al., 2019). The diurnal temperature range is generally lower dur-  
91 ing summer, and therefore affected by the elevated summer temperatures (Yang & Slingo,  
92 2001; Geerts, 2003). However, both seasonal and diurnal temperature variations over land  
93 depend strongly on local processes which are typically not well simulated by climate mod-  
94 els. There is therefore generally poor consistency across climate models and between ob-  
95 served and projected changes in both seasonal and diurnal tropical temperature varia-  
96 tions, especially on regional scales (Dwyer et al., 2012; C. Wang et al., 2014; Thorne, Do-  
97 nat, et al., 2016; Yin & Porporato, 2017; Chen et al., 2019; K. Wang & Clow, 2020).

98 Here we use the temperature-range definition of tropical climate land areas to ex-  
99 amine the extent of tropical land areas in reanalyses and in projections by coupled cli-  
100 mate models. Our methodology is described in Section 2, followed by our results and a  
101 discussion in Sections 3 and 4.

## 102 2 Data and methods

103 Observationally constrained data is taken from the European Center for Medium-  
104 Range Weather Forecasts (ECMWF) ERA5 reanalysis (0.25° X 0.25° resolution; Hers-  
105 bach et al., 2020), and from the National Aeronautics and Space Administration MERRA-  
106 2 reanalysis (0.625° X 0.5°; Gelaro et al., 2017) for the years 1980–2020.

107 The seasonal temperature range ( $\Delta_{Seasonal}$ ) is calculated as the difference between  
108 the months with hottest and coldest surface air temperatures (2m) in each year at each  
109 grid point. The diurnal temperature range ( $\Delta_{Diurnal}$ ) is calculated as the annual mean  
110 difference between monthly maximal and minimal diurnal surface temperatures at each  
111 grid point, derived from hourly data. We derive two parameters from the difference be-  
112 tween  $\Delta_{Diurnal}$  and  $\Delta_{Seasonal}$ : (i) Tropical land width is calculated as the distance be-  
113 tween the northern and southern latitudes where  $\Delta_{Diurnal} - \Delta_{Seasonal}$  changes sign;  
114 (ii) Tropical land area is calculated as the area-weighted sum over all land grid points  
115 in which  $\Delta_{Diurnal} > \Delta_{Seasonal}$  (lakes are excluded). For reference, the climatologies  
116 of observed seasonal and diurnal surface temperature ranges are shown and discussed  
117 in the Supporting Information (Figure S1).

118 We also analyze tropical temperature variations in 27 climate models from phase  
119 5 (Taylor et al., 2012) and 18 models from phase 6 (Eyring et al., 2016) of the Coupled  
120 Model Intercomparison Project (CMIP5/6), based on availability (Table S1). For CMIP5/6  
121 models,  $\Delta_{Seasonal}$  is calculated from monthly surface air temperature fields (i.e., the ‘tas’  
122 variable), and  $\Delta_{Diurnal}$  is calculated as the annual mean difference between monthly max-  
123 imal and minimal daily surface temperatures at each grid point (i.e., using the ‘tasmax’  
124 and ‘tasmin’ variables). For each model we use data only from the first realization (en-  
125 semble members ‘r1i1p1’ and ‘r1i1p1f1’ for CMIP5 and CMIP6, respectively), linearly  
126 interpolated to a common  $1.5^\circ \times 1.5^\circ$  horizontal grid.

127 To examine the relation of tropical land areas to the subtropical dry zones, we an-  
128alyze variations in precipitation minus evaporation ( $P - E$ ) in the 27 CMIP5 models  
129 and in 16 of the 18 CMIP6 models ( $P - E$  data is not available for the ‘GFDL-ESM4’  
130 and ‘CAS-ESM2-0’ models; see Table S1). Specifically, the poleward extent of the sub-  
131tropical dry zones increases with global warming, and is known to strongly covary with  
132 the width of the tropical meridional overturning circulation (Lu et al., 2007; Seviour et  
133 al., 2018). We calculate the poleward extent of the subtropical dry zones as the subtrop-

134 ical latitudes where the zonal mean  $P-E$  (over land and ocean) changes sign, averaged  
 135 over the northern and southern hemispheres, using the TropD software package (Adam  
 136 et al., 2018). (Note that this definition cannot be applied to only land areas, because evap-  
 137 oration nearly vanishes over land.) We also analyze the width of the tropical rain belt  
 138 (or the width of the intertropical convergence zone), which is projected to decrease under  
 139 global warming (Byrne & Schneider, 2016b). We estimate the width of the tropical  
 140 rain belt (TRB) as the standard deviation of the meridional distribution of precipita-  
 141 tion equatorward of  $20^\circ$ , which is well correlated with other indices of the TRB width  
 142 (Adam et al., 2022, see the Appendix for details). We apply this definition to the zonal  
 143 mean precipitation (over land and ocean), as well as to precipitation zonally averaged  
 144 over land.

145 To gauge model biases, we compare historical simulations averaged over the period  
 146 1980–1999 with the ERA5 and MERRA-2 reanalyses. For assessing the sensitivity to global  
 147 warming, we take the averaged difference between years 2080–2099 in the RCP85 (CMIP5)  
 148 and SSP585 (CMIP6) scenarios, in which pre-industrial  $\text{CO}_2$  levels are quadrupled by  
 149 the end of the 21st century, and the historical simulations. As shown in Figure S2, the  
 150 zonally land-averaged representation of  $\Delta_{Seasonal}$  and  $\Delta_{Diurnal}$  in the two CMIP phases  
 151 is statistically indistinguishable; we therefore analyze the two phases jointly. We note  
 152 that CMIP5/6 models are known to have regional biases in seasonal temperature vari-  
 153 ability, mainly associated with coupled large-scale circulation (C. Wang et al., 2014; Chen  
 154 et al., 2019), as well as deficiencies in the representation of diurnal temperature varia-  
 155 tions, associated with biases in cloud, surface, and vegetation processes (Yin & Porpo-  
 156 rato, 2017; K. Wang & Clow, 2020).

### 157 3 Results

#### 158 3.1 Zonal mean trends

159 Figure 2a compares  $\Delta_{Seasonal}$  and  $\Delta_{Diurnal}$  in the CMIP5/6 historical simulations  
 160 and in the ERA5 and MERRA-2 datasets, zonally averaged over land. In the subtropi-  
 161 cal latitudes where  $\Delta_{Diurnal} - \Delta_{Seasonal}$  changes sign, the model seasonal temperature  
 162 ranges are in broad agreement with the reanalyses. However, diurnal temperature ranges  
 163 do not agree across both models and reanalyses, for example in the southern hemisphere  
 164 where the models underestimate  $\Delta_{Diurnal}$  (more so when compared with MERRA-2),  
 165 reflecting the large uncertainty in simulating diurnal temperature variations (K. Wang  
 166 & Clow, 2020). We therefore proceed with the analysis while acknowledging the large  
 167 uncertainties associated with changes in diurnal temperature variations. In addition, given  
 168 the discrepancies across reanalyses and the significant role of natural variability in ob-  
 169 served tropical widening trends (Nguyen et al., 2013; Adam et al., 2014; Staten et al.,  
 170 2018), our analysis hereon focuses only on long-term trends associated with global warm-  
 171 ing in CMIP5/6 projections.

172 Figure 2b shows the CMIP5/6 ensemble means of  $\Delta_{Seasonal}$  and  $\Delta_{Diurnal}$ , zonally  
 173 averaged over land, in historical simulations and in projections. The projected changes  
 174 show: (i) generally increased tropical  $\Delta_{Seasonal}$ , and (ii) reduced  $\Delta_{Diurnal}$  in the north-  
 175 ern hemisphere and increased  $\Delta_{Diurnal}$  in the southern hemisphere, suggesting an over-  
 176 all decrease in the extent of tropical land area. Consistent with previous analyses, since  
 177  $\Delta_{Seasonal}$  increases with mean temperature, the projected increase in  $\Delta_{Seasonal}$  is caused  
 178 by enhanced warming during the warm season (e.g., Chen et al., 2019).

179 Figure 3a,b shows model probability distribution functions (PDFs) of the projected  
 180 changes per 1K global warming of tropical land width (mean latitudinal extent of land  
 181 where  $\Delta_{Diurnal} > \Delta_{Seasonal}$ ) and of tropical land area (net land area where  $\Delta_{Diurnal} >$   
 182  $\Delta_{Seasonal}$ ). A shift toward reduced tropical width and area is seen in nearly all of the  
 183 models, indicating a reduced net tropical extent under global warming (ensemble mean

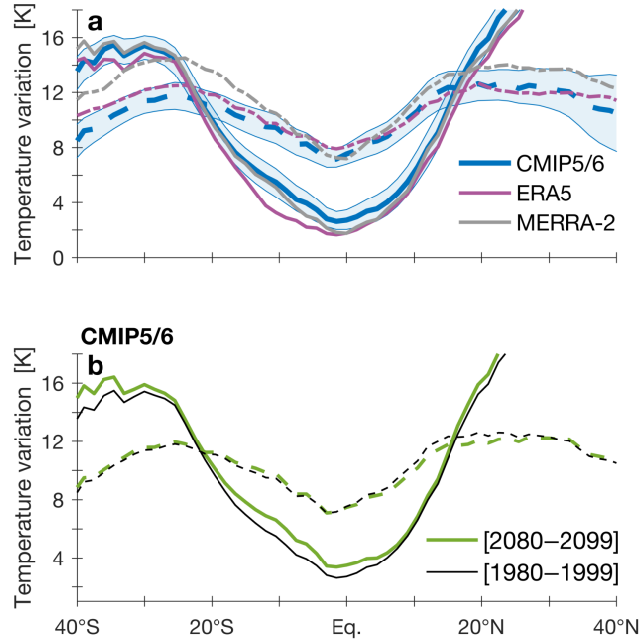


**Figure 2.** (a) Amplitudes of seasonal ( $\Delta_{Seasonal}$ , solid) and diurnal ( $\Delta_{Diurnal}$ , dashed) surface temperature ranges, zonally averaged over land, for CMIP5/6 historical simulations (blue) and for the ERA5 (purple) and MERRA-2 (gray) reanalyses. Shading indicates  $\pm 1$  standard deviation across models. (b) Ensemble mean CMIP5/6 values of  $\Delta_{Diurnal}$  and  $\Delta_{Seasonal}$ , zonally averaged over land, for the periods 1980–1999 (black, historical simulations) and 2080–2099 (green, RCP85/SSP585 simulations).

184 decrease in width and area per 1K is  $0.48^\circ$  and  $0.78 \cdot 10^6 \text{ km}^2$ ; see Figure S3 for the cor-  
 185 responding end of 20th and end of 21st centuries' PDFs).

186 Figure 3c,d shows the projected changes in the poleward extent of the subtropi-  
 187 cal dry zones (SDZs) and in the width of the tropical rain belt (TRB), zonally averaged  
 188 over land and ocean. A clear poleward expansion of the SDZs is seen, associated with  
 189 a widening of the tropical meridional overturning circulation (, e.g., Seviour et al., 2018;  
 190 Waugh et al., 2018), and a narrowing of the TRB, associated with increased energy trans-  
 191 port out of the rising branch of the tropical overturning circulation (Byrne & Schneider,  
 192 2016a). These changes indicate an expansion of the SDZs on both their poleward and  
 193 equatorward edges (Byrne & Schneider, 2016a). However, as shown in Figure 3e, there  
 194 is no statistically significant change in the width of the TRB over land. The narrowing  
 195 of tropical climate land area is therefore not clearly related to the expansion of the sub-  
 196 tropical descending zones, which is attributed to changes in the tropical meridional over-  
 197 turning circulation, but is manifested primarily over ocean due to confounding effects  
 198 by land-ocean temperature contrast and radiative forcing (He & Soden, 2017).

### 199 3.2 Regional trends

200 We now turn to examine regional changes. Given the similarities between the width  
 201 and area indices, and given that tropical zonally-varying width is not well defined in nar-  
 202 row continent strips (Figure 1b), we focus our regional analysis on tropical land area.

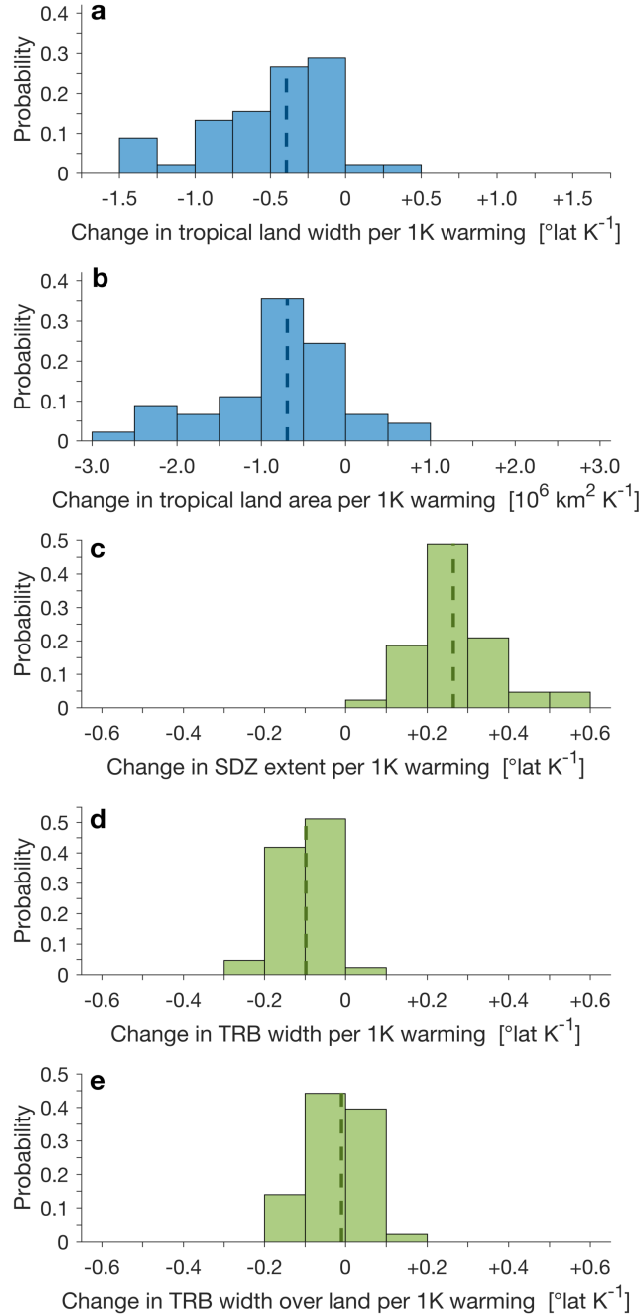


**Figure 3.** Probability distribution functions of changes per 1K global mean temperature warming in (a) tropical land width (mean latitudinal extent of land where  $\Delta_{Diurnal} > \Delta_{Seasonal}$ ), (b) tropical land area (net land area where  $\Delta_{Diurnal} > \Delta_{Seasonal}$ ), (c) extent of the zonal mean (over land and ocean) subtropical dry zones (SDZs), (d) width of the zonal mean tropical rain belt (TRB), and (e) width of the TRB averaged over land. Vertical lines show medians. The PDFs are composed of 45 models in panels a and b, and of 43 models in panels c–e.

203 Figure 4a shows the projected ensemble-mean changes per 1K warming in  $\Delta_{Diurnal} -$   
 204  $\Delta_{Seasonal}$ . Significant reduction of tropical land area is seen over Africa and the Amer-  
 205 icas, and to a lesser degree over the Asian and western Pacific sectors (see Figures S4

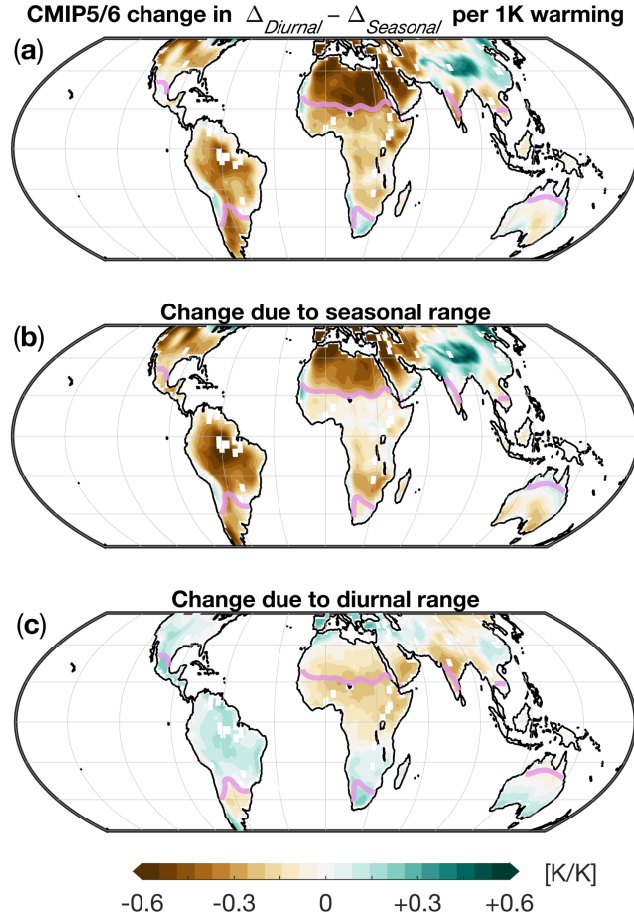


**Figure 4.** Change in  $\Delta_{Diurnal} - \Delta_{Seasonal}$  in the CMIP5/6 ensemble mean per 1K global mean temperature warming. (a) total change; (b) change due to  $\Delta_{Seasonal}$  (i.e.,  $\Delta_{Diurnal}$  is held fixed); (c) change due to  $\Delta_{Diurnal}$  (i.e.,  $\Delta_{Seasonal}$  is held fixed). Pink lines show latitudes where  $\Delta_{Diurnal} - \Delta_{Seasonal} = 0$ .

206 and S5 for PDFs of the regional changes). Specifically, the ensemble-mean projected regional changes in tropical land area per 1K are  $-0.31 \cdot 10^6 \text{ km}^2$  over Africa,  $-0.43 \cdot 10^6 \text{ km}^2$   
 207 over the Americas, and  $-0.03 \cdot 10^6 \text{ km}^2$  over Asia and the western Pacific sectors.  
 208

209 The specific contributions of changes in  $\Delta_{Seasonal}$  and  $\Delta_{Diurnal}$  are shown in Figure 4b,c. Most of the reduction in net tropical land area is due to increased  $\Delta_{Seasonal}$ ,  
 210 with  $\Delta_{Diurnal}$  having a generally small reinforcing effect over northern Africa, and a balancing effect elsewhere. Therefore, despite the large uncertainties in projected changes  
 211 in the diurnal temperature range, the reduction of tropical land area is a robust response to global warming, associated primarily with increased seasonal temperature range in  
 212 the tropics.  
 213  
 214  
 215

216 Since the increased seasonal temperature range is associated with reduced evaporative cooling during summer (Sobel & Camargo, 2011; Chen et al., 2019), we examine  
 217 the ensemble-mean changes in precipitation minus evaporation ( $P-E$ ), normalized per 1K global warming, in Figure 5. Drying is consistent with increased seasonal temperature  
 218 range over northern America and southern Africa. But it is likely not a key driver of the increased temperature range in the already-dry northern Africa, and in the wet-  
 219  
 220  
 221

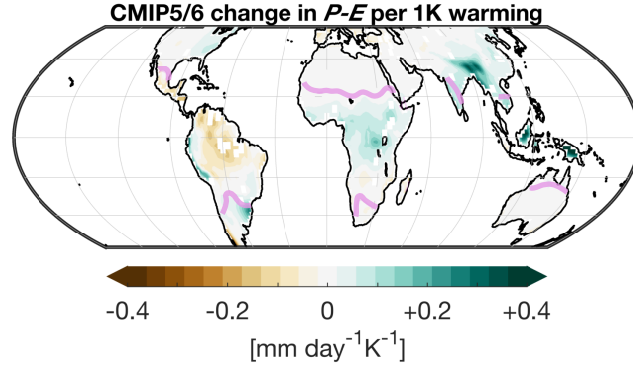


**Figure 5.** CMIP5/6 ensemble mean projected changes in precipitation minus evaporation ( $P - E$ ) over land per 1K warming. Pink lines show latitudes where  $\Delta_{Diurnal} - \Delta_{Seasonal} = 0$ .

222 ter southern America and parts of the Asian sector. Thus, the decreased extent of trop-  
 223 ical land areas, as defined here, cannot be generally attributed to drying.

#### 224 4 Discussion

225 Tropical climate land areas can be defined as regions where the diurnal surface tem-  
 226 perature range exceeds the seasonal surface temperature range (Figure 1). Based on this  
 227 definition we find a robust reduction of tropical land area with global warming in a  
 228 cohort of 27 CMIP5 and 18 CMIP6 models forced with high-emission scenarios.

229 The projected decrease in tropical land area is driven primarily by an increased sea-  
 230 sonal temperature range (Figure 2b), consistently seen across regions (Fig. 4b), caused  
 231 by enhanced summer warming (Sobel & Camargo, 2011; Chen et al., 2019). The di-  
 232 urnal temperature range generally decreases in the northern hemisphere and increases in  
 233 the southern hemisphere (Figure 2b), and has an overall small contribution to the changes  
 234 in tropical land area (Figure 4c). Thus, despite large uncertainties in simulated trends  
 235 of the diurnal temperature range, the reduction of tropical land area with global warm-  
 236 ing is a robust response, seen in nearly all of the CMIP5/6 models (Figure 3a,b).

237 The net loss of tropical land area with global warming coincides with the projected  
 238 expansion of the subtropical descending zones on both their equatorward and poleward  
 239 edges (Lu et al., 2007; Lau & Kim, 2015), associated with dynamic processes, and with  
 240 the projected global expansion of drylands, due to increased aridity (Huang et al., 2017).  
 241 However, the reduction in tropical land area is not clearly related to either of these dy-  
 242 namic and thermodynamic trends. Specifically, the expansion of the subtropical descend-  
 243 ing zones is caused by the widening of the mean meridional overturning circulation (MOC),  
 244 which is also observed across regions (Grise et al., 2018; Staten et al., 2019; D’Agostino  
 245 et al., 2020), and the narrowing of the width of the tropical rain belt (i.e., the rising branch  
 246 of the MOC Byrne & Schneider, 2016b; Byrne et al., 2018; Donohoe et al., 2019). But  
 247 the width of the tropical rain belt does not decrease over land, and is therefore not clearly  
 248 related to changes in the MOC (Figure 3). Similarly, changes in the seasonal and di-  
 249 urnal temperature ranges are not directly related to changes in precipitation minus evap-  
 250 oration (Figure 5). Moreover, in the subtropics, where tropical climate land area is lost,  
 251 CMIP5 models project transitions of land areas from both wet-to-drier and from dry-  
 252 to-wetter conditions (Figure 5; Feng & Fu, 2013; Grünzweig et al., 2022). Therefore, dy-  
 253 namic and thermodynamic drivers likely have diverse effects on the reduction in trop-  
 254 ical climate land area. Further analysis is required to to better understand the causes  
 255 and implications of reduced tropical land area, especially on regional to local scales.

## Appendix A Width of the tropical rain belt

Defining the centroid latitude of the meridional distribution of zonal-mean precipitation  $P$  as

$$\phi_{cent} = \int_{20^{\circ}S}^{20^{\circ}N} P(\phi)\phi \cos(\phi)d\phi, \quad (\text{A1})$$

the width of the tropical rain belt (TRB) is estimated as the standard deviation of the meridional distribution of precipitation,

$$W_{TRB} = \left[ \frac{\int_{20^{\circ}S}^{20^{\circ}N} P(\phi)(\phi - \phi_{cent})^2 \cos(\phi)d\phi}{\int_{20^{\circ}S}^{20^{\circ}N} P(\phi) \cos(\phi)d\phi} \right]^{\frac{1}{2}}. \quad (\text{A2})$$

This width estimate is generally correlated with other TRB width indices across CMIP5/6 models (Adam et al., 2022), and can be consistently applied to global and over-land zonal averages of precipitation. Results based on this estimate are also not statistically different from those obtained using TRB width defined as the difference between the northern and southern hemisphere precipitation centroids, used by Donohoe et al. (2019). Other indices of TRB width which rely on the meridional mass streamfunction or geometric quantities of the precipitation distribution (Popp & Lutsko, 2017; Byrne et al., 2018) cannot be applied over land due to the regional and irregular precipitation distributions.

## Data availability statement

All of the data used in the analyses presented here is publicly available. We thank the climate modeling groups for producing and making available their model output, the Earth System Grid Federation (ESGF) for archiving the data and providing access, and the multiple funding agencies who support CMIP and ESGF. All CMIP data analyzed here are available from the ESGF at <https://esgf-node.llnl.gov/projects/esgf-llnl>. The CMIP5 and CMIP6 models used can be found in Table S1

## Acknowledgments

OA acknowledges support by ISF grant 1022/21.

## References

- Adam, O., Farnsworth, A., & Lunt, D. J. (2022). Modality of the tropical rain belt across models and simulated climates. *Journal of Climate*(10.1175/JCLI-D-22-0521.1), –.
- Adam, O., Grise, K. M., Staten, P., Simpson, I. R., Davis, S. M., Davis, N. A., . . . Ming, A. (2018). The TropD software package (v1): standardized methods for calculating tropical-width diagnostics. *Geosci. Model Dev.*, *11*, 4339-4357. doi: 10.5194/gmd-11-4339-2018
- Adam, O., Schneider, T., & Harnik, N. (2014). Role of changes in mean temperatures versus temperature gradients in the recent widening of the Hadley circulation. *J. Climate*, *27*, 7450-7461.
- Bony, S., Stevens, B., Frierson, D. M. W., Jakob, C., Kageyama, M., Pincus, R., . . . Webb, M. J. (2015). Clouds, circulation and climate sensitivity. *Nature Geosci.*, *8*, 261–268.
- Byrne, M. P., Pendergrass, A. G., Rapp, A. D., & Wodzicki, K. R. (2018). Response of the intertropical convergence zone to climate change: Location, width, and strength. *Current Climate Change Reports*, *4*(4), 355–370. doi: 10.1007/s40641-018-0110-5

- 296 Byrne, M. P., & Schneider, T. (2016a). Energetic constraints on the width of the inter-  
297 tropical convergence zone. *J. Climate*, *29*, 4709–4721.
- 298 Byrne, M. P., & Schneider, T. (2016b). Narrowing of the itcz in a warming climate:  
299 Physical mechanisms. *Geophysical Research Letters*, *43*(21), 11–350.
- 300 Chen, J., Dai, A., & Zhang, Y. (2019). Projected changes in daily variability  
301 and seasonal cycle of near-surface air temperature over the globe during the  
302 twenty-first century. *Journal of Climate*, *32*(24), 8537–8561.
- 303 D’Agostino, R., Scambiati, A. L., Jungclaus, J., & Lionello, P. (2020). Poleward  
304 shift of northern subtropics in winter: Time of emergence of zonal versus re-  
305 gional signals. *Geophysical Research Letters*, *47*(19), e2020GL089325.
- 306 Donohoe, A., Atwood, A. R., & Byrne, M. P. (2019). Controls on the width of trop-  
307 ical precipitation and its contraction under global warming. *Geophysical Re-  
308 search Letters*, *46*(16), 9958–9967.
- 309 Donohoe, A., & Battisti, D. S. (2013). The seasonal cycle of atmospheric heating  
310 and temperature. *J. Climate*, *26*, 4962–4980.
- 311 Dwyer, J. G., Biasutti, M., & Sobel, A. H. (2012). Projected changes in the seasonal  
312 cycle of surface temperature. *Journal of Climate*, *25*(18), 6359–6374.
- 313 Eyring, V., Bony, S., Meehl, G. A., Senior, C. A., Stevens, B., Stouffer, R. J., &  
314 Taylor, K. E. (2016). Overview of the coupled model intercomparison project  
315 phase 6 (cmip6) experimental design and organization. *Geoscientific Model  
316 Development*, *9*(5), 1937–1958.
- 317 Feng, S., & Fu, Q. (2013). Expansion of global drylands under a warming climate.  
318 *Atmospheric Chemistry and Physics*, *13*(19), 10081–10094.
- 319 Geerts, B. (2003). Empirical estimation of the monthly-mean daily temperature  
320 range. *Theoretical and Applied Climatology*, *74*(3), 145–165.
- 321 Gelaro, R., McCarty, W., Suárez, M. J., Todling, R., Molod, A., Takacs, L., . . .  
322 others (2017). The modern-era retrospective analysis for research and applica-  
323 tions, version 2 (merra-2). *Journal of climate*, *30*(14), 5419–5454.
- 324 Grise, K. M., Davis, S. M., Staten, P. W., & Adam, O. (2018). Regional and sea-  
325 sonal characteristics of the recent expansion of the tropics. *Journal of Climate*,  
326 *31*(17), 6839–6856.
- 327 Grünzweig, J. M., De Boeck, H. J., Rey, A., Santos, M. J., Adam, O., Bahn, M., . . .  
328 others (2022). Dryland mechanisms could widely control ecosystem functioning  
329 in a drier and warmer world. *Nature Ecology & Evolution*, 1–13.
- 330 He, J., & Soden, B. J. (2017). A re-examination of the projected subtropical precipi-  
331 tation decline. *Nature Climate Change*, *7*(1), 53–57.
- 332 Hersbach, H., Bell, B., Berrisford, P., Hirahara, S., Horányi, A., Muñoz-Sabater, J.,  
333 . . . others (2020). The era5 global reanalysis. *Quarterly Journal of the Royal  
334 Meteorological Society*, *146*(730), 1999–2049.
- 335 Holmes, C. R., Woollings, T., Hawkins, E., & De Vries, H. (2016). Robust fu-  
336 ture changes in temperature variability under greenhouse gas forcing and the  
337 relationship with thermal advection. *Journal of Climate*, *29*(6), 2221–2236.
- 338 Huang, J., Li, Y., Fu, C., Chen, F., Fu, Q., Dai, A., . . . others (2017). Dryland cli-  
339 mate change: Recent progress and challenges. *Reviews of Geophysics*, *55*(3),  
340 719–778.
- 341 Lau, W. K., & Kim, K.-M. (2015). Robust hadley circulation changes and increas-  
342 ing global dryness due to co2 warming from cmip5 model projections. *Proceed-  
343 ings of the National Academy of Sciences*, *112*(12), 3630–3635.
- 344 Lu, J., Vecchi, G. A., & Reichler, T. (2007). Expansion of the Hadley  
345 cell under global warming. *Geophys. Res. Lett.*, *34*, L06805.  
346 (doi:10.1029/2006GL028443)
- 347 Manabe, S., Ploshay, J., & Lau, N.-C. (2011). Seasonal variation of surface temper-  
348 ature change during the last several decades. *Journal of climate*, *24*(15), 3817–  
349 3821.
- 350 Nguyen, H., Evans, A., Lucas, C., Smith, I., & Timbal, B. (2013). The Hadley

- 351 circulation in reanalyses: Climatology, variability, and change. *J. Climate*, *26*,  
352 3357–3376.
- 353 Nguyen, H., Hendon, H., Lim, E.-P., Bosch, G., Maloney, E., & Timbal, B. (2018).  
354 Variability of the extent of the hadley circulation in the southern hemisphere:  
355 a regional perspective. *Climate Dynamics*, *50*(1), 129–142.
- 356 Paffen, K. (1967). Das verhältnis der Tages-zur jahreszeitlichen Temper-  
357 aturschwankung: Erläuterungen zu einer neuen Weltkarte als Beitrag zur  
358 allgemeinen Klimageographie (the relationship of diurnal to annual tempera-  
359 ture variations). *Erdkunde*, *XXI*, 94–111.
- 360 Palmer, T., & Stevens, B. (2019). The scientific challenge of understanding and  
361 estimating climate change. *Proceedings of the National Academy of Sciences*,  
362 *116*(49), 24390–24395. doi: 10.1073/pnas.1906691116
- 363 Popp, M., & Lutsko, N. (2017). Quantifying the zonal-mean structure of tropical  
364 precipitation. *Geophysical Research Letters*, *44*(18), 9470–9478.
- 365 Riehl, H. (1954). *Tropical meteorology* (Tech. Rep.). McGraw-Hill.
- 366 Riehl, H., et al. (1979). *Climate and weather in the tropics*. Academic Press.
- 367 Ruane, A., Ranasinghe, R., Vautard, R., Arnell, N., Coppola, E., Cruz, F. A., ...  
368 others (2021). Ipcc ar6 wgi chapter 12: Climate change information for re-  
369 gional impact and for risk assessment. In *Agu fall meeting abstracts* (Vol. 2021,  
370 pp. U13B–12).
- 371 Seidel, D. J., Fu, Q., Randel, W. J., & Reichler, T. J. (2008). Widening of the tropi-  
372 cal belt in a changing climate. *Nature Geosci.*, *1*, 21–24.
- 373 Seviour, W. J., Davis, S. M., Grise, K. M., & Waugh, D. W. (2018). Large uncer-  
374 tainty in the relative rates of dynamical and hydrological tropical expansion.  
375 *Geophysical Research Letters*, *45*(2), 1106–1113.
- 376 Sobel, A. H., & Camargo, S. J. (2011). Projected future seasonal changes in tropical  
377 summer climate. *Journal of Climate*, *24*(2), 473–487.
- 378 Staten, P. W., Grise, K. M., Davis, S. M., Karlsruh, K., & Davis, N. (2019).  
379 Regional widening of tropical overturning: Forced change, natural variability,  
380 and recent trends. *Journal of Geophysical Research: Atmospheres*, *124*(12),  
381 6104–6119.
- 382 Staten, P. W., Grise, K. M., Davis, S. M., Karlsruh, K. B., Waugh, D. W., May-  
383 cock, A. C., ... Son, S.-W. (2020, 06). Tropical Widening: From Global  
384 Variations to Regional Impacts. *Bulletin of the American Meteorological Soci-  
385 ety*, *101*(6), E897-E904. doi: 10.1175/BAMS-D-19-0047.1
- 386 Staten, P. W., Lu, J., Grise, K. M., Davis, S. M., & Birner, T. (2018). Re-examining  
387 tropical expansion. *Nature Climate Change*, *8*(9), 768–775.
- 388 Stine, A. R., & Huybers, P. (2012). Changes in the seasonal cycle of temperature  
389 and atmospheric circulation. *Journal of Climate*, *25*(21), 7362–7380.
- 390 Stouffer, R., & Wetherald, R. (2007). Changes of variability in response to increas-  
391 ing greenhouse gases. part i: Temperature. *Journal of Climate*, *20*(21), 5455–  
392 5467.
- 393 Taylor, K. E., Stouffer, R. J., & Meehl, G. A. (2012). An overview of cmip5 and  
394 the experiment design. *Bulletin of the American meteorological Society*, *93*(4),  
395 485–498.
- 396 Thorne, P., Donat, M., Dunn, R., Williams, C., Alexander, L., Caesar, J., ... others  
397 (2016). Reassessing changes in diurnal temperature range: Intercomparison  
398 and evaluation of existing global data set estimates. *Journal of Geophysical  
399 Research: Atmospheres*, *121*(10), 5138–5158.
- 400 Thorne, P., Menne, M., Williams, C., Rennie, J., Lawrimore, J., Vose, R., ... others  
401 (2016). Reassessing changes in diurnal temperature range: A new data set and  
402 characterization of data biases. *Journal of Geophysical Research: Atmospheres*,  
403 *121*(10), 5115–5137.
- 404 Troll, C. (1943). Thermische klimatypen der Erde (thermal climate types of Earth).  
405 *Petermanns Geogr. Mitteil.*, *43*(3/4), 81–89.

- 406 Wang, C., Zhang, L., Lee, S.-K., Wu, L., & Mechoso, C. R. (2014). A global per-  
407 spective on cmip5 climate model biases. *Nature Climate Change*, *4*(3), 201–  
408 205.
- 409 Wang, K., & Clow, G. D. (2020). The diurnal temperature range in cmip6 mod-  
410 els: Climatology, variability, and evolution. *Journal of Climate*, *33*(19), 8261–  
411 8279.
- 412 Waugh, D., Grise, K. M., Seviour, W., Davis, S., Davis, N., Adam, O., . . . Simpson,  
413 I. R. (2018). Revisiting the relationship among metrics of tropical expansion.  
414 *J. Climate*.
- 415 Wild, M. (2009). Global dimming and brightening: A review. *Journal of Geophysical*  
416 *Research: Atmospheres*, *114*(D10).
- 417 Yang, G.-Y., & Slingo, J. (2001). The diurnal cycle in the tropics. *Monthly Weather*  
418 *Review*, *129*(4), 784–801.
- 419 Yettella, V., & England, M. R. (2018). The role of internal variability in twenty-  
420 first-century projections of the seasonal cycle of northern hemisphere surface  
421 temperature. *Journal of Geophysical Research: Atmospheres*, *123*(23), 13–149.
- 422 Yin, J., & Porporato, A. (2017). *Diurnal cloud cycle biases in climate models, nat.*  
423 *commun.*, *8*, 2269.